International Journal of Scientific Research Updates

Journal homepage: https://orionjournals.com/ijsru/

ISSN: 2783-0160 (Online)

(RESEARCH ARTICLE)

Check for updates

The formation young's modulus and textural attributes of the Axx-field from southern Niger delta, Nigeria

Joseph Gordian ATAT, Emmanuel Bassey UMOREN *, Akaninyene Okon AKANKPO and Joyce Ime ISAIAH

Department of Physics, University of Uyo, Uyo, Nigeria.

International Journal of Scientific Research Updates, 2024, 07(01), 009–028

Publication history: Received on 09 November 2023; revised on 02 January 2024; accepted on 05 January 2024

Article DOI: https://doi.org/10.53430/ijsru.2024.7.1.0076

Abstract

This research was carried out to determine the formation brittleness and textural attributes of an Axx-Field in the Niger Delta Basin. Data available for this study were obtained from three wells (A11, A22 and A33). They were analyzed using Microsoft Excel after spurious values were removed. Two techniques (John Fuller and Plumb Bradford) were used to determine static young's modulus but only one is reported because after statistical analysis on both, the one reported was adequate for accurate outcomes although both approaches have low variance. The results indicates that the highest values of static and dynamic young's modulus are 2.05 x 1025N/m2 and 1.93 x 1010N/m2 respectively. The lowest values are 1.1 x 1024N/m2 and 8.5 x 109N/m2 respectively for well A11. The average values are 1.024 x 1025N/m2 and 5.25 x 1023N/m2 for this well. For well A22, the highest and lowest values of dynamic young's modulus are 1.5848 x 1010N/m2 and 1.5726 x 1010N/m2 while those of static are correspondingly 1.47 x 1025N/m2 and 9.01 x 1014N/m2. Their average values are 1.5787 x 1010N/m2 and 7.35 x 1024N/m2 for dynamic and static young's moduli respectively. Also, for well A33, dynamic has the lowest value as 3.28 x 1010 N/m2; static has 8.36 x 1014N/m2 and their highest correspond to 2.04 x 1010N/m2 and 7.08 x 1025N/m2. The average value for this well are 2.66 x 1010N/m2 and 3.54 x 1025 N/m2 for dynamic and static respectively. The static Young's modulus results define the formation as brittle, whose environment is extremely poorly sorted, very fine skewed and very leptokurtic with low energy for well A11, very poorly sorted, fine skewed and platykurtic for well A22, extremely poorly sorted, very fine skewed and mesokurtic for well A33.

Keywords: Young's modulus; Gamma ray; Textural parameters; Sorting; Skewness; Percentile; Velocity; Shear modulus

1 Introduction

Brittleness defines the property of a material that fractures when it is stressed but has a slight tendency to deform before rupture (Zhang, 2011). Young's modulus is an elastic mechanical rock characteristic that shows a stones resistance of the layer to uniaxial load. It is one of the brittleness evaluation parameters and can be quantified through extracted rock elastic properties. Other parameters are Poisson 's ratio and lame's parameters. Young's modulus is vital in the static drilling of hydrocarbon wells since it helps to describe the formation and total stresses, which is utilized to manage well bore instability. The mechanical properties (mainly including elastic moduli and strength) of rocks play a significant role in the hydraulic fracturing of reservoirs in terms of initiating and propagating the fractures (Josh *et al.*, 2012) and thus impact both the efficiency of the fracturing methods and the flow of hydrocarbons to the well bore (Eliyahu *et al*., 2015). Using the elastic and strength properties of rock, a variety of brittleness indices may be noted to quantitatively evaluate rock brittleness, which can be used to access the favorability of reservoirs for fracturing operation (Grieser and Bray, 2007). Brittleness is a critical indicator for hydraulic fracturing candidate screening in unconventional reservoirs. The areas with high young's modulus and low Poisson's ratio are more productive for

* Corresponding author: Umoren E. B

hydraulic fracturing due to their high brittleness. Static young's modulus changes greatly with the different of the lithology. For shale, the static Young's modulus varies from 0.1Mpsi to 0.99Mpsi. It ranges from 8 and 12Mpsi in limestone and 2 to 10Mpsi in sandstone. These differences in young's modulus values emphasize that this characteristic changes with lithology, making it essential in prediction of the static young modulus along hydrocarbon wells. Probability of failure rises with depth in deep wells (deeper than 1500 meters).

Geomechanical properties of rocks are either statically or dynamically measured. Static measurement has to do with the use of core specimens in the laboratory, where the core specimens are exposed to incremental compression until they undergo fracture while recording the stress-strain curve. The dynamic mechanical properties can be obtained using p-wave velocities from seismic, well logs or laboratory-analyzed core data (Al-Shayea, 2004; Hongzhi, 2005; Chang *et al*., 2006; Xu *et al*., 2016). To avoid frequent drilling challenges relative to wellbore stability, precise description of the geomechanical properties of a rock is necessary. Sonic and density logs may be employed in determining the dynamic mechanical properties of a reservoir rock which include bulk modulus, young's modulus, Poisson's ratio and shear modulus, in order to obtain static mechanical properties leading to the estimation of rock strength properties (Archer and Rasouli, 2012; Najibi *et al*., 2015; Xu *et a*l., 2016). Dynamic moduli values are usually less than their equivalent static moduli, and as such the ratio of dynamic moduli to static moduli gets smaller with increasing confining pressures, while their difference increases in tight sands and shale reservoirs (Adham, 2016).

Grieser and Bray (2007), suggested a brittleness index, using young's modulus and Poisson's ratio stating that rocks with a high young's modulus and low Poisson's ratio will be brittle. Britt and Schoeffler (2009), concluded that shale with a static young's modulus larger than 3.5 × 106 psi (approximately 20.684 Gpa) will be brittle. According to Maleki *et al*. (2014), the previous method of evaluating young's modulus by means of acoustic velocities revealed that the larger the acoustic velocity, corresponding to the larger density, the larger the elastic property of rocks. Static elastic moduli are preferred over moduli obtained using dynamic approaches (Eissa and kazi, 1988); this is based on the theory of the pseudo-static behavior of rock.

The focus of this research is on young's modulus information and textural attributes beginning from sonic log by converting the compressional interval transit time to p-wave velocities and then applying well established empirical relations (Archer and Rasouli, 2012; Słota-Valim, 2013, 2015; Jamshidian *et al*., 2017). The clear advantage of this method over measurement of static properties directly, using uniaxial loading test is that, it is less destructive to the specimen, more cost effective and time efficient (Zhang and Bentley, 2005). The p-wave, and s-wave, velocities are the inverse of interval transit times (Brandås, 2012; Horsfall *et al*., 2014; Schön, 2015).

1.1 Theoretical background

Young's Modulus or Elastic Modulus or Tensile Modulus, is the measurement of mechanical properties of linear elastic solids like rods, wires, and other which include Bulk modulus and Shear modulus but the value of Young's Modulus is mostly used. This is due to the fact that it gives information about the tensile elasticity of a material. Mathematically, Young's modulus (E) may be expressed as in Equation 1.

$$E = \frac{Stress}{Strain} \quad \text{.....(1)}$$

According to Atat *et al*. (2022,), Young's Modulus may also be determined using Equation 2.

$$E = 2\mu(1 + \sigma) \quad \text{.....(2)}$$

Where, E is young's Modulus in Pa or Nm^{-2}
μ is Shear modulus
σ is Poisson's ratio

The value of Poisson's ratio ranges between -1 and 0.5 for most common materials. The minus sign indicates that the lateral strain is in the opposite direction to the axial strain.

A Poisson's ratio of 0 means that the material does not change in lateral dimensions when stretched or compressed. A positive value indicates that the material tends to expand laterally when stretched, while a negative value indicates that the material tends to contract laterally when stretched. Poisson's ratio is an important parameter in materials science and engineering, as it influences the material's mechanical behavior, such as its stiffness, deformability, and response to stress and strain.

Poisson's ratio may be determined using Equation 3 (Atat *et al*., 2020a; 2020b; Atat and Umoren 2016; Atat et al., 2023).

$$\sigma = \frac{\left(\frac{V_p}{V_s}\right)^2 - 2}{2\left(\frac{V_p}{V_s}\right)^2 - 1} \text{.....(3)}$$

Where σ is Poisson's ratio
V_S is Compressional wave velocity
V_s is Shear wave velocity

The shear modulus is a fundamental parameter that characterizes the stiffness and ability of a material to withstand deformation under shear loads. In the context of oil wells and reservoirs, the shear modulus plays a crucial role in understanding the mechanical behavior and stability of the formation rocks.

Equation 4 is adequate for shear modulus determination (Atat *et al*., 2012; Atat and Umoren 2016; Akpabio *et al*., 2023a).

$$\mu = \rho V_s^2 \text{.....(4)}$$

V_s is shear wave velocity

Bulk modulus is one of the mechanical properties used in several geoengineering problems (Wang et al., 2022; Bock, 1993; Bell, 1996; Andhumoudine et al 2021; Yang and Liu, 2021) and it could be obtained by the stress-strain relation (like static measurement) or the propagating elastic wave velocities (such as dynamic measurement) (Wang et al., 2020).

The static bulk modulus symbolizes the mechanical firmness of subsurface basins (Zimmer, 2004; Zoback, 2007). The dynamic moduli can be examined from seismic or well logging data (Fjaer, 2019; Wang et al., 2022). It may be determined using Equation 5.

$$K = \frac{E}{3\,(1-2\sigma)} \text{.....(5)}$$

K is Bulk modulus (Atat et al., 2020a)
σ is the Poisson ratio
E is the young's modulus

The Statistical/textural parameters include graphic mean, graphic standard deviation, graphic skewness and graphic kurtosis. They are required for grain size and statistical spreading. Textural parameters can be obtained from percentile deduction and statistical analysis of data. It relates with the velocity of the medium accountable for the transportation and deposition of sediment (or sand-shale lithology in this research) (Atat et al., 2018; Oladipo et al., 2018). Table 1 highlights different interpretation of these parameters with their corresponding values.

The mean (M) may be obtained using Equation 6.

$$M = \frac{1}{3}(\phi_{16} + \phi_{50} + \phi_{84}) \text{.....(6)}$$

Parameters such as standard deviation, sorting, skewness and kurtosis can be calculated using Equations 7 to 10 correspondingly.

Standard deviation (SD) is a measure of sorting. The sorting (S) of a given population is a measure of the range of grain-size present and the magnitude of these sizes around the mean sizes. SD and S expressions are presented in Equations 7 and 8 respectively.

$$SD = \frac{1}{4}(\phi_{84} - \phi_{16}) \text{.....(7)}$$

$$S = \frac{\phi_{84} - \phi_{16}}{4} + \frac{\phi_{95} - \phi_5}{6.6} \text{.....(8)}$$

Negatively skewed (which is coarse skewed) defines high energy environment and positively skewed (which is finely skewed) corresponds to low energy environment.

$$S_k = 0.5\left(\frac{\phi_{84}+\phi_{16}-2\phi_{50}}{\phi_{84}-\phi_{16}} + \frac{\phi_5+\phi_{95}-2\,\phi_{50}}{\phi_{95}-\phi_5}\right) \text{.....(9)}$$

(Atat et al., 2018; Oladipo et al., 2018; Folk and Ward, 1957; Atat et al., 2022; Adedoyin 2022; Gandhi and Raja, 2014).

Kurtosis measures the sorting ratio at the extremes of the distribution. If kurtosis is defined as platykurtic, its value is negative excess kurtosis (that is, opposite situation to the case of leptokurtic); if it is mesokurtic, kurtosis curve is observed to have uniform sorting in both tails and central position and finally leptokurtic, if its value is positive excess kurtosis (tail is better sorted than central portion). It is a quantitative measure used to describe the departure from normality of distribution. It signifies the ratio between sorting in tails and central portion of the curve. The calculation of Kurtosis could be done using Equation 10.

$$K_s = \frac{\emptyset_{95}-\emptyset_5}{2.44(\emptyset_{75}-\emptyset_{25})} \text{.....(10)}$$

Table 1 Classification of textural parameters (Atat et al., 2021; Oladipo et al., 2018; Atat et al., 2022; Wentworth, 1922)

S/N	Parameters	Range of values	Interpretation/Classification
1	Sorting	Less than 0.35	Very well sorted
2	Sorting	0.35 to 0.50	Well sorted
3	Sorting	0.51 to 0.70	Moderately well sorted
4	Sorting	0.71 to 1.00	Moderately sorted
5	Sorting	1.01 to 2.00	Poorly sorted
6	Sorting	2.01 to 4.00	Very poorly sorted
7	Sorting	Greater than 4.00	Extremely poorly sorted
8	Skewness	Less than - 0.30	Very coarse skewed
9	Skewness	- 0.30 to - 0.11	Coarse skewed
10	Skewness	- 0.10 to +0.10	Near symmetrical
11	Skewness	+0.11 to +0.30	Fine skewed
12	Skewness	Greater than +0.30	Very fine skewed
13	Kurtosis	Less than 0.67	Very platykurtic
14	Kurtosis	0.67 to 0.90	Platykurtic
15	Kurtosis	0.91 to 1.11	Mesokurtic
16	Kurtosis	1.12 to 1.50	Leptokurtic
17	Kurtosis	1.51 to 3.00	Very leptokurtic
18	Kurtosis	Greater than 3.00	Extremely leptokurtic

1.2 Coefficient of Variation (CV)

This is also called Relative Standard Deviation (RSD) which is the standardized measure of dispersion of probability or frequency distribution. It is the ratio of the SD to the mean signifying the extent of variability in relation to the mean population. If CV is less than one, it is low variance; if it is greater than one, it is high variance. It is mostly expressed in percentage (Atat et al., 2022).

1.3 Geology of the Area of Study

In the Niger Delta, **A_{xx}** Field is located, South of Port Harcourt, Rivers State, Nigeria. Niger Delta basin (Figure 1) is about latitudes 3^0N to 6^0N; longitudes 5^0E to 8^0E (Atat et al., 2020b; Akpabio et al., 2023a; Klett et al., 1997; Atat et al 2022; Akpabio et al., 2023b; Umoren et al., 2019). This region experiences wet and dry moments depending on the season in a year and the average rain in a month during wet season is about 1.35 x 10^2mm and reduces to 6.50 x 10^1mm while approaching dry season (Atat et al., 2020c; Atat et al., 2020d; George *et al*., 2017; Atat and Umoren, 2016). The volume of sediment is nearly 500000km^3. The oil in the basin belongs to the category of Akata-Agbada. More of marine shales made up the Akata formation with an expected width of up to 7.0 x 10^3m. The Agbada formation is the major oil reservoir in the Niger Delta (Atat et al., 2020c; Umoren et al., 2020; Udo *et al*., 2017; Atat et al., 2020e; Hospers, 1965).

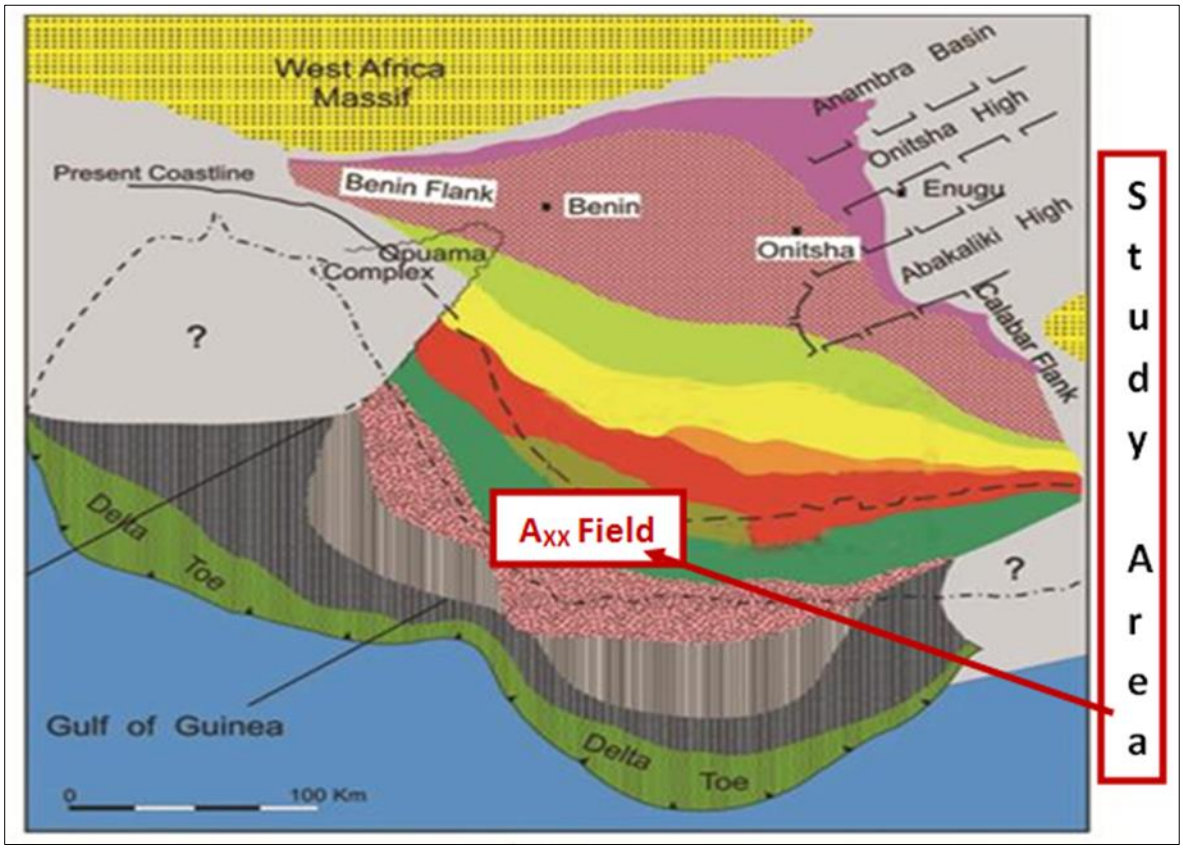

Figure 1 Map Showing the studied location

2 Materials and method

2.1 Material

Onshore **A_{xx}** Field data was acquired from the Niger Delta Basin. These include well location and raw well data. (Depth, Gamma ray, Sonic and Density). With Microsoft Excel, data loading, processing, plots/curves, diagrams and other computations were accomplished.

2.2 Method

Three wells (A_{11}, A_{22} and A_{33}) were studied. Suites of log such as depth, gamma ray, density and sonic were generated from the available data. These data were analyzed using Microsoft Excel. Figure 2 summaries the steps taken to attain at the goal.

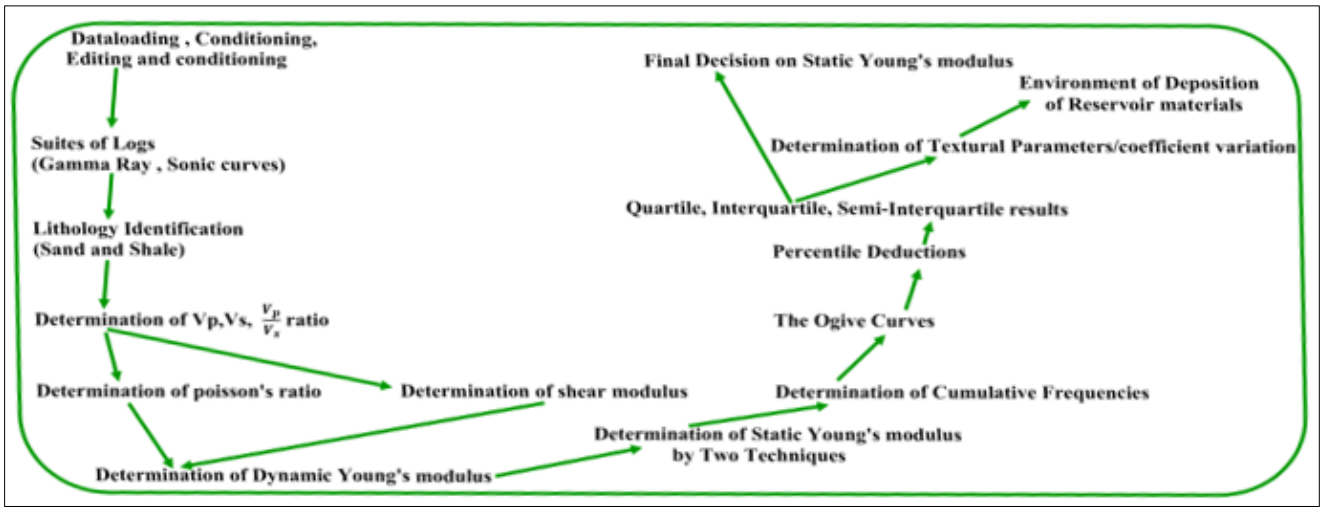

Figure 2 Workflow showing the analysis

3 Result

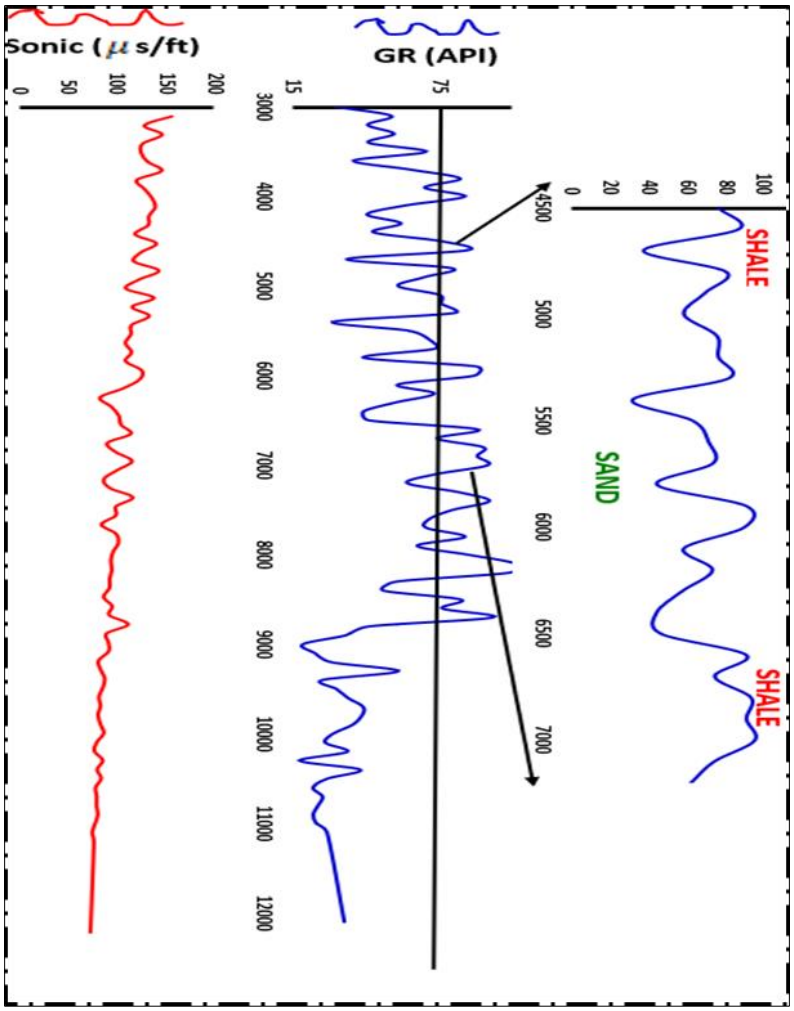

Figure 3 The generated suites of log with depth for gamma (blue) and sonic (red) indicating the sand/shale base line of Well A_{11}

This research was conducted to determine the young's modulus and define the reservoir materials in A_{XX} field. These well data were obtained and generated into suites of log indicating the sand/shale baseline as presented in Figures 3, 6 and 9 for wells A_{11}, A_{22}, and A_{33} respectively. Parameters (dependent variables) like compressional wave velocity, shear wave velocity, the ratio of these velocities was accounted for and shear modulus was determined. With the dependent variable information, Dynamic and Static young's moduli were obtained (Figures 4, 7 and 10). Figures 5, 8 and 11 highlight the variation of the result of static young's modulus with generated sonic curves. Figures 12, 13 and 14 became necessary in order to decide on a better static young's modulus result. Table 2 shows the result of the percentiles obtained from the two techniques employed. Table 3 indicates the textural attributes and interpretation of the formation.

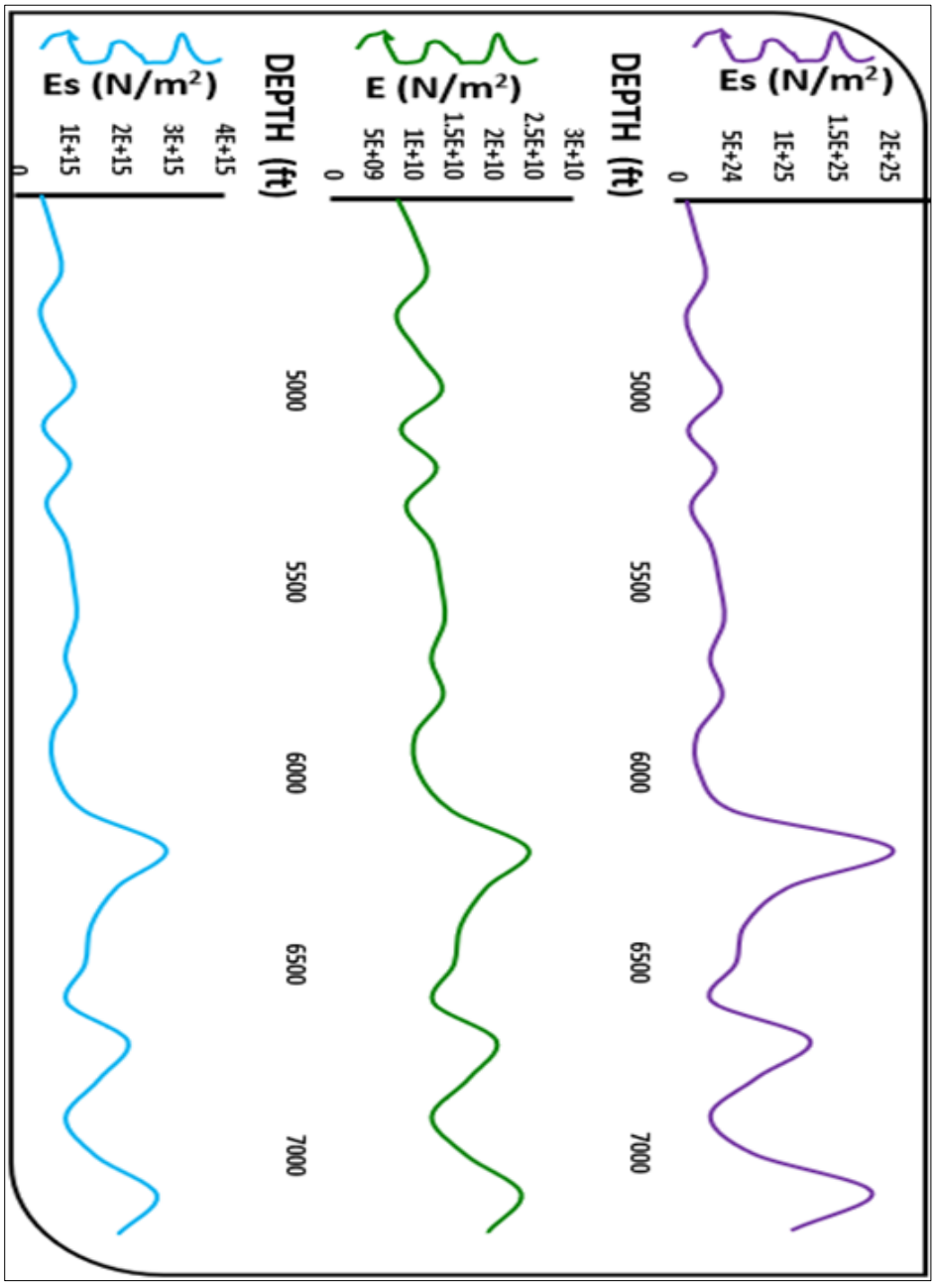

Figure 4 Young's modulus with depth curves (sky blue for static by AQ, green for dynamic and purple for static by AP) of well A_{11}

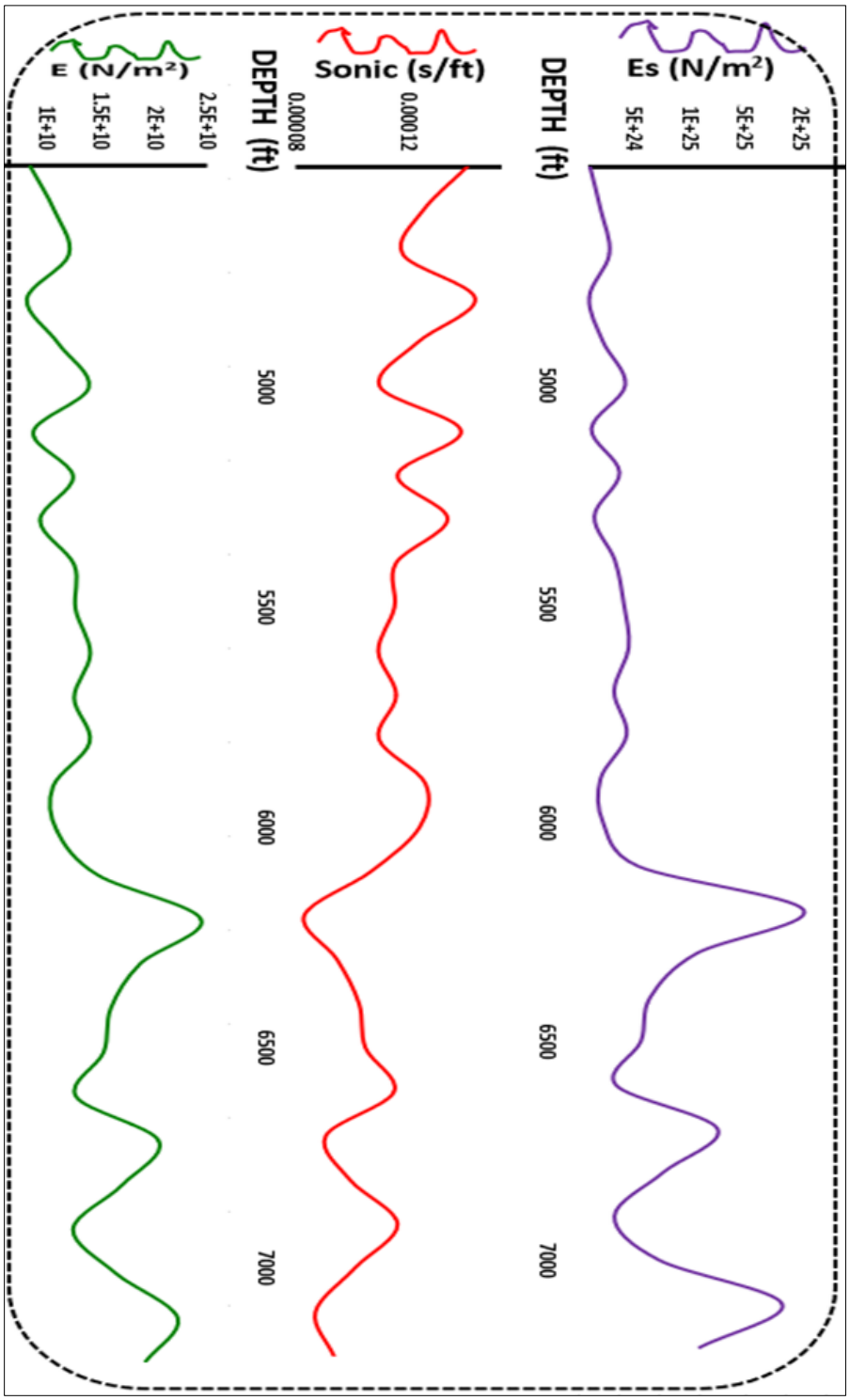

Figure 5 The relationship between young's moduli (green for dynamic and purple for static), sonic (red) and depth from well A_{11}

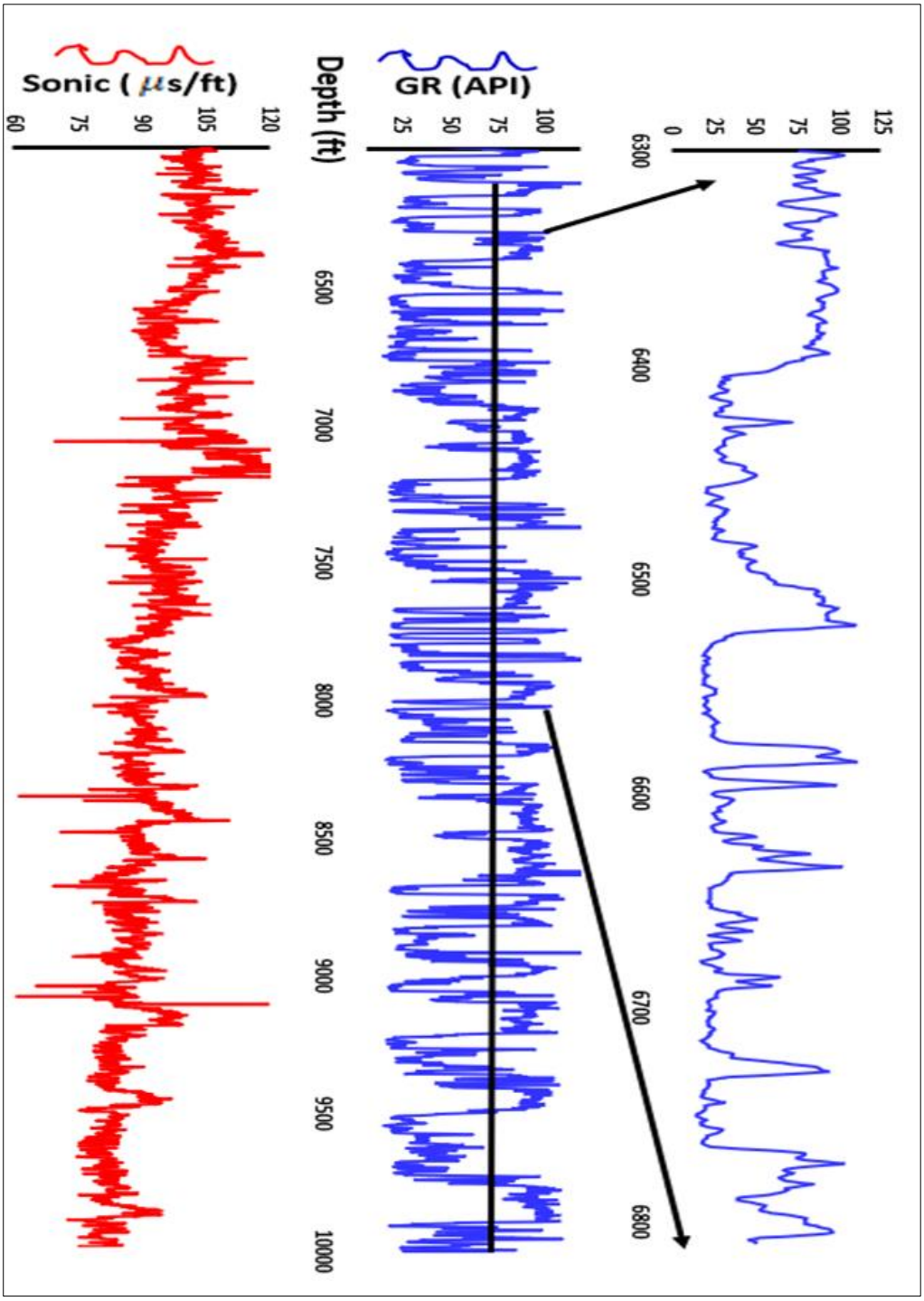

Figure 6 The generated suites of log with for gamma (blue) and sonic (red) indicating the sand/shale base line of Well A_{22}

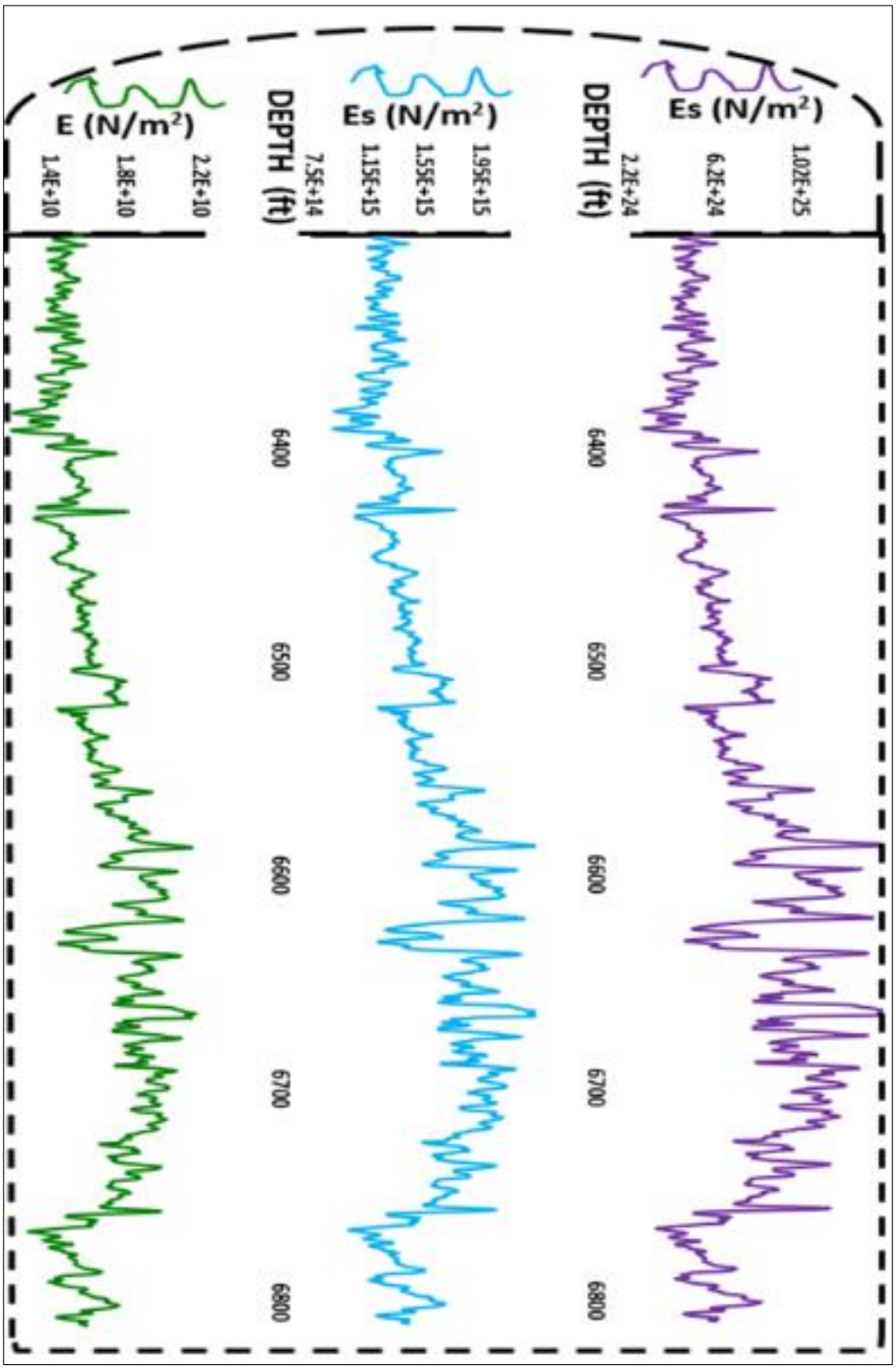

Figure 7 Young's modulus with depth curves (sky blue for static by AQ, green for dynamic and purple for static by AP) of well A_{22}

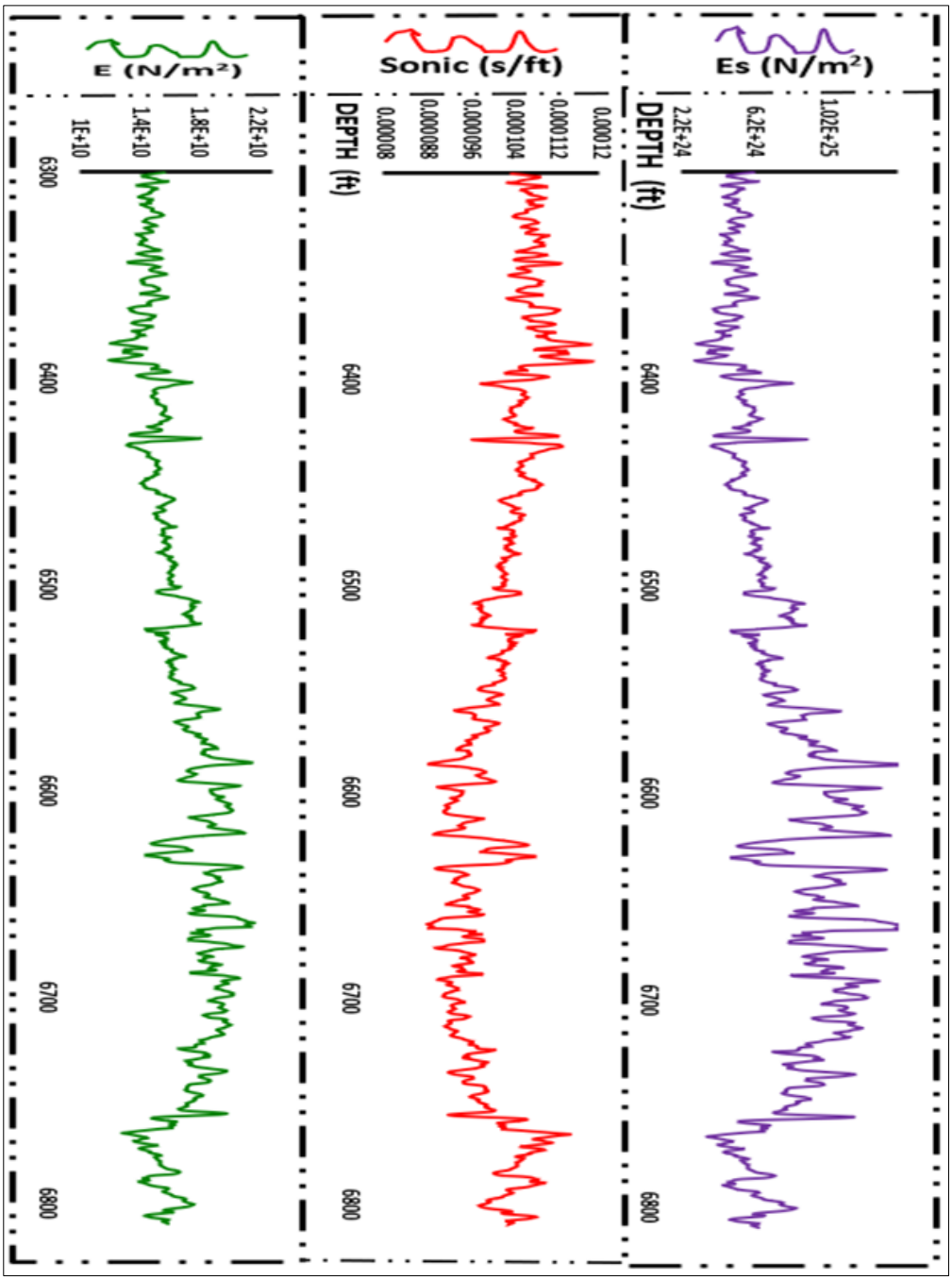

Figure 8 The relationship between young's moduli (green for dynamic and purple for static), sonic (red) and depth from well A_{22}

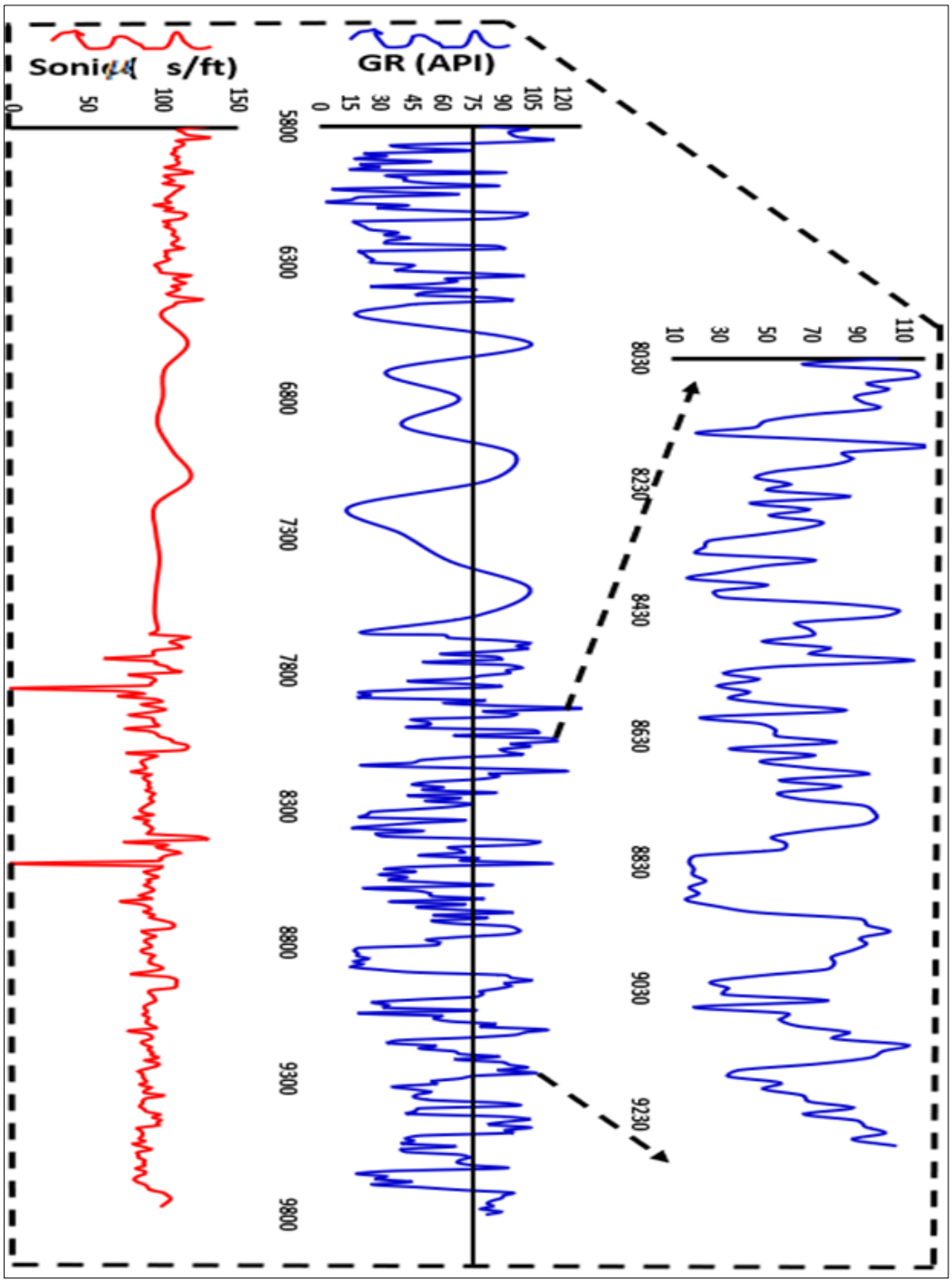

Figure 9 The generated suites of log with depth for gamma (blue) and sonic (red) indicating the sand/shale base line of Well A_{33}

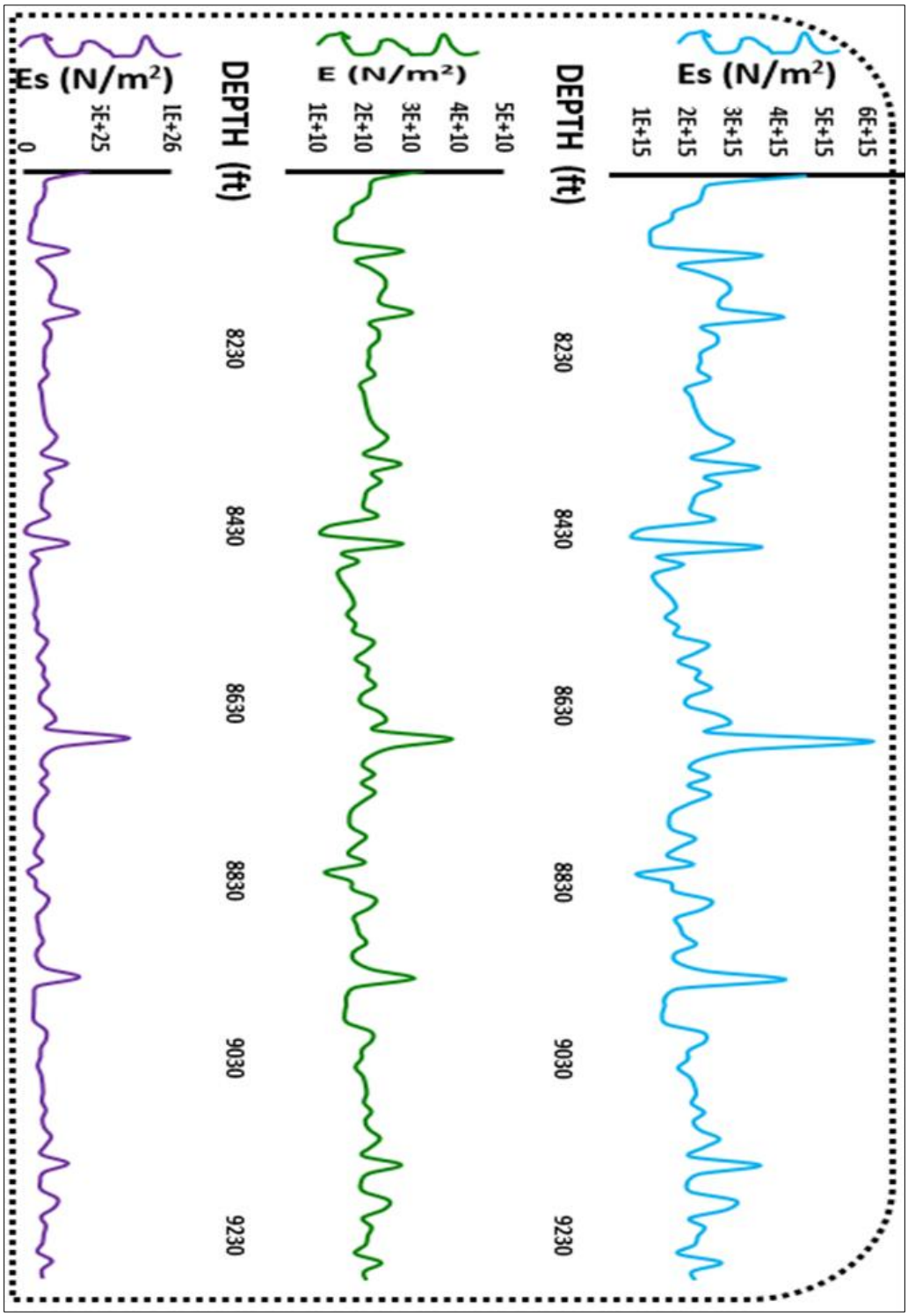

Figure 10 Young's modulus with depth curves (sky blue for static by AQ, green for dynamic and purple for static by AP) of well A_{33}

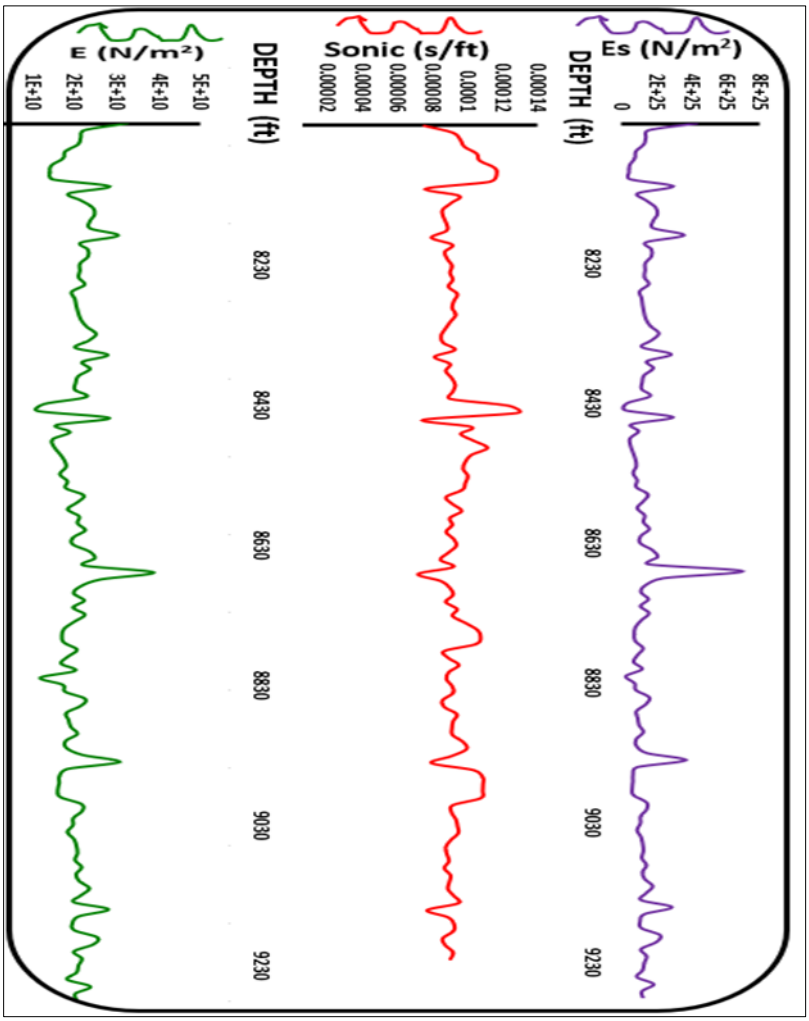

Figure 11 The relationship between young's moduli (green for dynamic and purple for static), sonic (red) and depth from well A_{33}

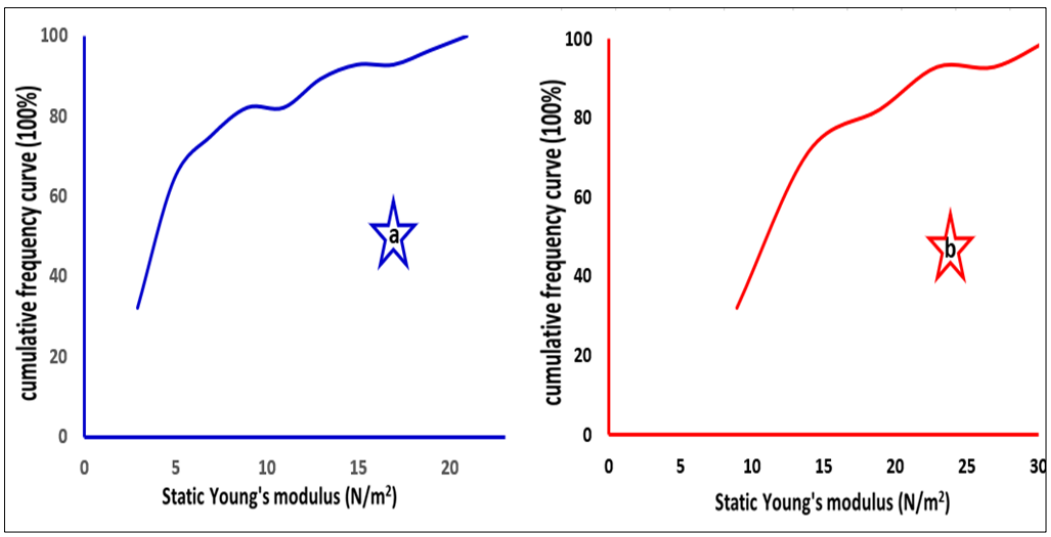

Figure 12 The Ogive resulting from Bradford technique (a) and Fuller technique (b) of Well A_{11}.

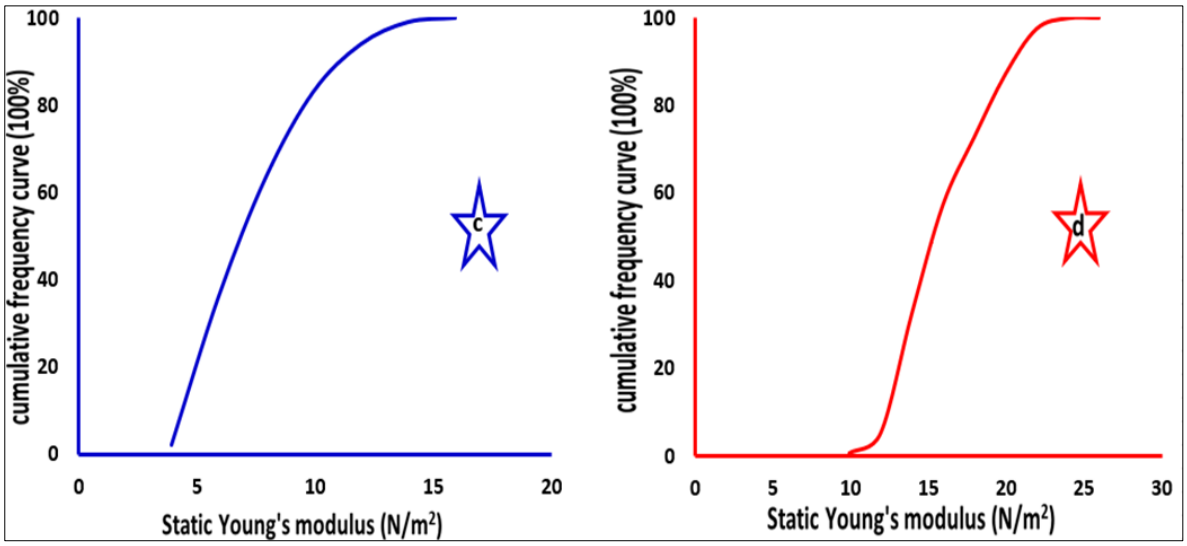

Figure 13 The Ogive resulting from Bradford technique (c) and Fuller technique (d) of Well A_{22}

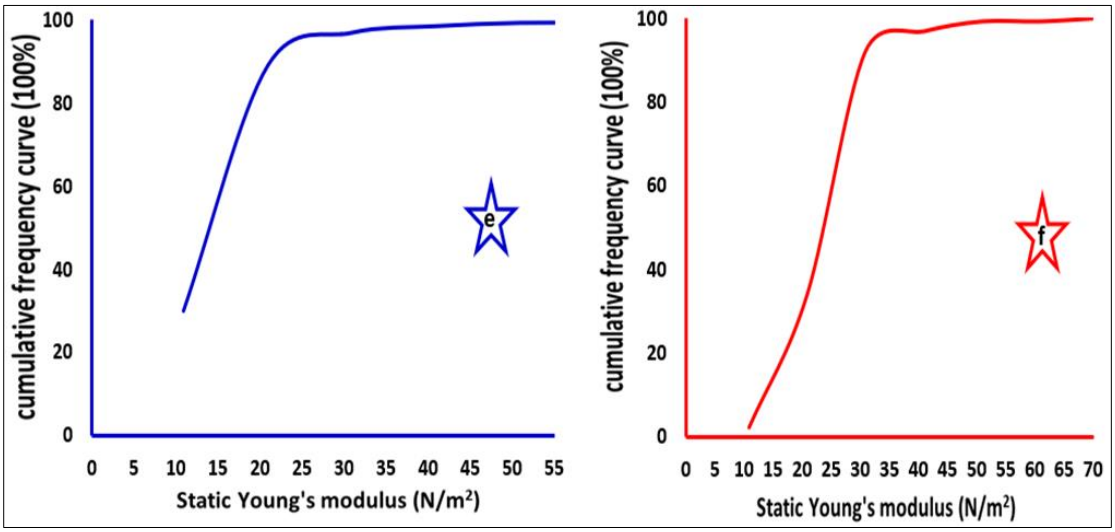

Figure 14 The Ogive resulting from Bradford technique (e) and Fuller technique (f) of Well A_{33}

Table 2 The Percentiles obtained from each Technique and other Statistical Results

Wells	Techniques	Percentiles							SD	Mean	CV
		ϕ_5	ϕ_{16}	ϕ_{25}	ϕ_{50}	ϕ_{75}	ϕ_{84}	ϕ_{95}			
A_{11}	Bradford	1.5	2.1	2.6	4.0	6.9	11.5	18.2	2.35	5.86666667	0.4006
	Fuller	6.2	7.3	8.1	11.0	14.7	19.6	28.4	3.075	12.6333333	0.2434
A_{22}	Bradford	4.1	4.7	5.2	6.8	9.0	10.0	12.2	1.325	7.16666670	0.1849
	Fuller	11.9	12.8	13.4	15.2	18.2	19.4	21.3	1.65	15.8000000	0.1044
A_{33}	Bradford	7.0	8.2	10.0	12.0	18.0	19.0	25.0	2.7	13.06666667	0.2066
	Fuller	11.0	15.0	18.2	23.0	27.0	29.0	32.0	3.5	22.33333333	0.1567

Table 3 The result of textural attributes and interpretation

Wells	Techniques	Sorting	skewness	Kurtosis	Interpretation
A_{11}	Bradford	4.8803	0.64817	1.591689	Extremely poorly sorted, very fine skewed, very leptokurtic
A_{11}	Fuller	6.43864	0.48297	1.378539	Extremely poorly sorted, very fine skewed, leptokurtic
A_{22}	Bradford	2.55227	0.27044	0.873598	very poorly sorted, fine skewed, platykurtic
A_{22}	Fuller	3.07424	0.2853	0.802596	very poorly sorted, fine skewed, platykurtic
A_{33}	Bradford	5.42727	0.37037	0.922131	Extremely poorly sorted, very fine skewed, mesokurtic
A_{33}	Fuller	6.68182	-0.1429	0.978018	Extremely poorly sorted, coarse skewed, mesokurtic

Table 4 The Interquartile Range and Semi-Interquartile Range result summary

	Well A_{11}		Well A_{22}		Well A_{33}	
Techniques	**Bradford**	**Fuller**	**Bradford**	**Fuller**	**Bradford**	**Fuller**
IQR	4.30	6.6	3.8	4.8	8.0	8.8
SIQR	2.15	3.3	1.9	2.4	4.0	4.4
Diff. M from Q3	2.90	3.7	2.2	3.0	6.0	4.0
Diff. M from Q1	1.40	2.9	1.6	1.8	2.0	4.8

4 Discussion

The data were loaded in Excel; spurious values were removed and suites of log generated for the three wells, with red colour signifying sonic and blue for Gamma ray (Figures 3, 6 and 9). The sand lithology and shale lithology were identified and marked as sand and shale where the Gamma ray index is about less than 75 API and greater than 75 API respectively. This thickness was considered and yielded more results about the reservoir, leading to young's modulus information.

Compressional wave velocity was determined from the sonic data. Shear wave velocity was determined using Castagna equation. $\frac{V_P}{V_S}$ ratio is a value Poisson's ratio depends on, so it was determined as well as Poisson's ratio (Equation 3 was adequate). Shear modulus was determined using Equation 4. The calculation of dynamic young's modulus was done with Equation 2. Two static young's moduli results were obtained using two approaches (Bradford and Fuller techniques). In order to settle for the most accurate results, percentile deductions of quartile and interquartile information were necessary. The cumulative frequencies were determined and ogive plotted (Figure 12 to 14) correspondingly for wells A_{11}, A_{22}, and A_{33}). Table 2 was computed from the ogive curves. The standard deviation and mean in Table 2 were calculated using Equations 7 and 6 respectively. Sorting, skewness and kurtosis were computed with Equations 8, 9 and 10 respectively. Table 1 was used for the interpretation.

4.1 For well A_{11},

The sand/shale investigated has a thickness of 2700ft (about 823m) which is from 4500ft to 7200ft. Red curve is for sonic, blue curve is for Gamma ray. The highest value of static young's modulus (2.048×10^{25} N/m^2) is noted at 6200ft indicating that it does not depend on the depth of the reservoir. The lowest value ($1.0\ 5x\ 10^{24}$N/m^2) is noted at 4800ft. For dynamic young's modulus, its highest value is (1.93×10^{10}N/m^2) at 6200ft and lowest value is (8.5×10^{9}N/m^2) at 4800ft. Therefore, increase in dynamic young's modulus leads to an increase in static young's modulus. This finding agrees with Figure 4. The sky blue is the static young's modulus from Fuller technique, green is dynamic young's modulus and purple represents static young's modulus from Bradford approach. Relating the final result of young's moduli with sonic log shows that increase in sonic information leads to a decrease in young's modulus. The choice of the most accurate result of static young's modulus was from the percentile deductions which involved Figure 12 and Table 2. Table 2 presents the values of IQR and SIQR obtained from Bradford approach as lower than those computed from Fuller technique. Moreso, Fuller values deviate strongly from the median than Bradford values. Table 3 defines the

reservoir environment as extremely poorly sorted, very fine skewed and very leptokurtic. With this information, it is a low energy environment. According to Britt and Schoeffler (2009), static young's modulus greater than 3.5 x 10^6 psi (which is about 20.684Gpa) will be brittle as one of the important elastic properties of rock. Since both the lowest and highest values of the static young's modulus obtained in this research is greater than this standard, therefore the reservoir rock is brittle. Brittleness refers to the ability of a material to fracture or break under stress without significant deformation. It is often used to characterize the mechanical behavior of rocks.

4.2 For well A_{22},

The sand/shale investigated has a thickness of 510ft (156m) which is from 6300ft to 6810ft. Red curve is for sonic, blue curve is for Gamma ray. The highest value of static young's modulus (1.47 x $10^{25}N/m^2$) is noted at 6664ft indicating that it does not depend on the depth of the reservoir. The lowest value (9.01315 x $10^{14}N/m^2$) is noted at 6391ft. For dynamic young's modulus, its highest value is (1.5848x$10^{10}N/m^2$) at 6664ft and lowest value is (1.5726 x $10^{10}N/m^2$) at 6391ft. Therefore, increase in dynamic young's modulus leads to an increase in static young's modulus. this finding agrees with Figure 7. The sky blue is the static young's modulus by Fuller technique, green is dynamic young's modulus and purple represents static young's modulus by Bradford approach. Relating the final result of young's moduli with sonic log shows that increase in sonic information leads to a decrease in young's modulus. The choice of the most accurate result of static young's modulus was from the percentile deductions which involved Figure 13 and Table 2; Table 2 values of IQR and SIQR obtained from Bradford approach are lower than those computed from Fuller technique. Moreso, Fuller values deviate strongly from the median than Bradford values. Table 3 defines the reservoir environment as very poorly sorted, fine skewed and platykurtic. With this information, it is a low energy environment. Britt and Schoeffler (2009), stated that static young's modulus greater than 3.5 x 10^6 psi (which is about 20.684Gpa) will be brittle as one of the important elastic properties of rock. Since both the lowest and highest values of the static young's modulus obtained in this research are greater than this standard, the reservoir rock is brittle. Brittleness refers to the ability of a material to fracture or break under stress without significant deformation. It is often used to characterize the mechanical behavior of rocks. Brittle materials are solid materials that tend to fracture or break under stress without significant deformation.

4.3 For well A_{33}

The sand/shale investigated has a thickness of 1250ft (about 381m) which is from 8030ft to 9280ft. Red curve is for sonic, blue curve is for Gamma ray. The highest value of static young's modulus (7.08 x 10^{25} N/m^2) is noted at 8670ft indicating that it does not depend on the depth of the reservoir. The lowest value (8.36x$10^{14}N/m^2$) is noted at 8440ft. For dynamic young's modulus, its highest value is (2.04 x $10^{10}N/m^2$) at 8670ft and lowest value is (3.28 x $10^{10}N/m^2$) at 8440ft. Therefore, increase in dynamic young's modulus leads to an increase in static young's modulus. this finding agrees with Figure 10. The sky blue is the static young's modulus by Fuller technique, green is dynamic young's modulus and purple represents static young's modulus by Bradford approach. Linking the final result of young's moduli with sonic log shows that increase in sonic information leads to a decrease in young's modulus. the choice of the most accurate result of static young's modulus was from the percentile deductions which involved Figure 14 and Table 2. The values of IQR and SIQR (Table 2) obtained from Bradford approach are lower than those computed from Fuller technique. Moreso, Fuller values deviate strongly from the median than Bradford values. Table 3 defines the reservoir environment as extremely poorly sorted, very fine skewed and mesokurrtic. Therefore, it is a low energy environment. Britt and Schoeffler (2009) findings indicated that static young's modulus greater than 3.5 x 10^6 psi (which is about 20.684Gpa) will be brittle as one of the important elastic properties of rock. Since both the lowest and highest values of the static young's modulus obtained in this research is greater than this standard, therefore the reservoir rock is brittle. Brittleness refers to the ability of a material to fracture or break under stress without significant deformation. It is often used to characterize the mechanical behavior of rocks.

Young's modulus is typically used to characterize the stiffness of solid materials and their response to applied stress and strain. The Coefficient of Variation (CV) is low in both techniques but the choice of a better technique was derived from the deviation from the median.

5 Conclusion

The young's modulus increases with a decrease in sonic. It is not influenced by the depth. Static young's modulus increases with increase in dynamic young's modulus. The result obtained classifies this elastic property as brittle. The wells would certainly stand a test of time without collapsed. The textural parameters defined the formation as brittle whose environment is extremely poorly sorted, very fine skewed and very leptokurtic with low energy for well A_{11}, very poorly sorted, fine skewed and platykurtic for well A_{22}, extremely poorly sorted, very fine skewed and mesokurtic for well A_{33}.

Compliance with ethical standards

Acknowledgments

The authors would like to express their appreciation to Professor Idara Akpabio of the Department of Geoscience, University of Uyo, Nigeria for the release of the data used in this study. Acknowledgement is made to the Reviewers for their inputs. We also thank the Editorial board of International Journal of Scientific Research Updates for the acceptance and publication of our article.

Disclosure of conflict of interest

No conflict of interest to be disclosed.

Statement of ethical approval

The Author confirms that the work described has not been published before; that it is not under consideration for publication elsewhere; that its publication has been approved by all co-authors; the copyright is transferred when the article is accepted for publication. The corresponding author signs for and accepts responsibility for releasing this material on behalf of any and all co-authors. The copyright transfer covers the exclusive right to reproduce and distribute the article.

Statement of Informed consent

Informed consent was obtained from all individual participants included in the study. The Authors consent to participate in the research project and the outcome of our investigation result in this article. The participation of the Authors is completely voluntary and they have agreed to publish this finding in International Journal of Scientific Research Updates as a research article.

References

[1] Adedoyin, A. D., Lekan-Ojo, K. A., Atat, J. G. and Omorinoye, O. A. (2022): Investigation of Textural Attributes of Sediment in Ifelodun County, Nigeria. World Journal of Applied Science and Technology, 14(1b): 97-106.

[2] Adham, A. (2016): Geomechanics Model for Wellbore Stability Analysis in Field" X" North Sumatra Basin. (PhD), Colorado School of Mines. Arthur Lakes Library.

[3] Akpabio, I. O., Atat, J. G. and Akankpo, A. O. (2023a): Local Fit Parameter Satisfying Shear Modulus Porosity Relation for Southern Z Basin Analysis. Neuroquantology, 21(5): 1385-1391.

[4] Akpabio, I. O., Atat, J. G., Umoren, E. B. and Ekemini, J. D. (2023b): The Reservoir Rock Volumetric Concentration and Tortuosity Description of Pore Space of Xa Field, Niger Delta Basin. World Journal of Advanced Science and Technology, 3(01): 1–13.

[5] Al-Shayea, N. A. (2004): Effects of Testing Methods and Conditions on the Elastic Properties of Limestone Rock. Engineering Geology, 74(1-2): 139-156.

[6] Andhumoudine, A., Nie, B., Zhou, Q.X., (2021): Investigation of Coal Elastic Properties Based on Digital Core Technology and Finite Element Method. Advances in Geo-Energy Research, 5(1): 53- 63.

[7] Archer, S., and Rasouli, V. (2012): A Log Based Analysis to Estimate Mechanical. Petroleum and Mineral Resources, 163-170.

[8] Atat, J. G., Essiett, A. A., Ekpo, S. S. and Umar, S. (2023): Modelling of Bulk Modulus from Sand [API <75]-Shale [API >75] Lithology for XA Field in the Niger Delta Basin. World Journal of Advanced Research and Reviews, 18(03): 635–644.

[9] Atat, J. G., Akpabio, I. O. and Ekpo, S. S. (2022): Percentile-Ogive Approach determine as the Textural parameter of Xa Field. Current Science, 2(5): 230-240.

[10] Atat, J. G. Adedoyin, A. D. and Umo, E. (2021): Discriminant Function and Critical Shear Stress Investigations Differentiate Depositional Environment in the Western Part of Nigeria. Journal of University of Babylon for Pure and Applied Sciences (JUBPAS), 29(3): 109-125.

[11] Atat, J. G., George, N. J. and Atat, A. G. (2020a): Immediate Settlement of Footing using Interpreted Seismic Refraction Geoelastic Data: A Case Study of Eket County, Nigeria. Nriag Journal of Astronomy and Geophysics, 9(1): 433–448.

[12] Atat, J. G., Uko, E. D., Tamunobereton-ari, I. and Eze, C. L. (2020b). The Constants of Density-Velocity Relation for Density Estimation in Tau Field, Niger Delta Basin. IOSR Journal of Applied Physics (IOSR-JAP), 12(1): 19 – 26. 29.

[13] Atat, J. G., Uko, E. D., Tamunobereton-ari, I. and Eze, C. L. (2020c). Site-Dependent Geological Model for Density Estimation in the Niger Delta Basin, Nigeria. Malaysian Journal of Geoscience (MJG), 4(1): 1 – 6. 31.

[14] Atat, J. G., Akankpo, A. O., Umoren, E. B., Horsfall, O. I. and Ekpo, S. S. (2020d). The Effect of Density-velocity Relation Parameters on Density Curves in Tau (τ) Field, Niger Delta Basin. Malaysian Journal of Geosciences (MJG), 4(2), 54-58.

[15] Atat, J. G., Horsfall, O. I. and Akankpo, A. O. (2020e): Density Modelling from Well Analysis of Fields [Sand API < 75 and Shale API > 75, Niger Delta Basin. IOSR Journal of Applied Geology and Geophysics (IOSR-JAGG), 8(2): 1-6.

[16] Atat, J. G. and Umoren, E. B. (2016): Assessment of Mechanical and Elastic Properties of Soils in the South Eastern Part of Niger Delta, Nigeria. World Journal of Applied Science and Technology, 8 (2), 188-193.

[17] Atat, J. G., Akpabio, G. T., George, N. J. and Umoren, E. B. (2012): Geophysical Assessment of Elastic Constants of Top Soil using Seismic Refraction Compressional Velocities in the Eastern Niger Delta. International Journal of Modern Physics, 1(1): 7 – 19.

[18] Atat, J., Oluwafemi, B. and Adedoyin, A. (2018): Kinetic Energy and Transportation History of Sediments in Ogunniyi, Western Nigeria. World Journal of Applied Science and Technology, 10 (2): 98 -109.

[19] Bell, J. S. (1996): In situ Stresses in Sedimentary Rocks (part 2), Applications of Stress Measurements. Geoscience, 23, 135-153.

[20] Bock, H. (1993): Measuring in Situ Rock Stress by Borehole Slotting. Principles, Practice and Projects, 3, 433-443.

[21] Brandås, L. T. (2012). Relating Acoustic Wave Velocities to Formation Mechanical Properties. Institutt for Petroleumsteknologi Og Anvendt Geofysikk.

[22] Britt, L.K. and Schoeffler, J., (2009): The Geomechanics of a Shale Play: what makes a Shale Prospective. SPE Eastern Regional Meeting, Charleston, West Virginia, 23–25, P. 9.

[23] Chang, C., Zoback, M. D. and Khaksar, A. (2006): Empirical Relations between Rock Strength and Physical Properties in Sedimentary Rocks. Journal of Petroleum Science and Engineering, 51(3-4): 223-237.

[24] Eissa, E.A. and Kazi, A. (1988): Relation between Static and Dynamic Young's Moduli of Rocks. International Journal of Rock Mechanics and Mining Sciences and Geomechanics Abstracts 25(6): 479–482.

[25] Eliyahu, M., Emmanuel, S., Day-Stirrat, R.J. and Macaulay C.I. (2015): Mechanical Properties of Organic Matter in Shales Mapped at the Nanometer Scale. Marine and Petroleum Geology 59, 294–304.

[26] Ellis, D.V., (1987): Well Logging for Earth Scientists. Elsevier. New York P.74-83.

[27] Fjaer, E. (2019). Relations between Static and Dynamic Moduli of Sedimentary Rocks. Geophysical Prospecting, 67(1): 128 -139.

[28] Folk, R. L. and Ward, W. C. (1957). Brazos River Bar: a Study in the Significance of Grain Size Parameter. Journal of Sedimentary Petrology, 27: 3-27.

[29] Gandhi, M. S. and Raja, M. (2014): Heavy Mineral Distribution and Geochemical Studies of Coastal Sediments between Besant Nagar and Marakkanam, Tamil Nadu, India. Journal of Radiation Research and Applied Sciences, 7(3): 256 – 268.

[30] George, N. J., Atat, J. G., Udoinyang, I. E., Akpan, A. E. and George, A. M. (2017). Geophysical Assessment of Vulnerability of Surficial Aquifer in the Oil Producing Localities and Riverine Areas in the Coastal Region of Akwa Ibom State, Southern Nigeria. Current Science, 113(3), 430-438.

[31] Grieser, W.V. and Bray, J. M., (2007): Identification of Production Potential in Unconventional Reservoirs. Production and Operations Symposium, Oklahoma, USA, 31 March-3 April, 2007. Society of Petroleum Engineers, P. 6.

[32] Hongzhi, L. B. B. (2005): Advances in Calculation Methods for Rock Mechanics Parameters. Petroleum Drilling Techniques, 5, 011.

[33] Horsfall, O., Omubo-Pepple, V., and Tamunobereton-ari, I. (2014): Estimation of Shear Wave Velocity for Lithological Variation in the North-Western Part of the Niger Delta Basin of Nigeria. American Journal of Scientific and Industrial Research, 5(1): 13-22.

[34] Hospers, J. (1965). Gravity Field and Structure of the Niger Delta, Nigeria, West Africa. Geological Society of American Bulletin, 76, 407 – 422. 30.

[35] Jamshidian, M., Zadeh, M. M., Hadian, M., Nekoeian, S. and Zadeh, M. M. (2017): Estimation of Minimum Horizontal Stress, Geomechanical Modeling and Hybrid Neural Network Based on Conventional Well Logging Data–a Case Study. Geosystem Engineering, 20(2): 88-103.

[36] Josh, M., Esteban L., Piane C.D., Sarout J., Dewhurst D.N. and Clennell M.B. (2012): Laboratory Characterization of Shale Properties. Journal of Petroleum Science and Engineering 88–89(2): 107–124.

[37] Klett, T. R., Ahlbrandt, T. S., Schmoker, J. W. and Dolton, J. L. (1997). Ranking of the World's Oil and Gas Provinces by Known Petroleum Volumes. United State Geological Survey Open-File Report, 97: 463. 25.

[38] Maleki, S., Gholami, R., Rasouli, V., Moradzadeh, A., Riabi, R.G. and Sadaghzadeh, F., (2014): Comparison of different Failure Criteria in Prediction of Safe Mud Weigh Window in Drilling Practice. Earth-Science Reviews 136(3): 36-58

[39] Najibi, A. R., Ghafoori, M., Lashkaripour, G. R. and Asef, M. R. (2015): Empirical Relations Between Strength and Static and Dynamic Elastic Properties of Asmari and Sarvak Limestones, Two Main Oil Reservoirs in Iran. Journal of Petroleum Science and Engineering, 126, 78-82.

[40] Oladipo, V. O., Adedoyin, A. D. and Atat, J. G. (2018). The Geostatistical Investigation of Grain Size and Heavy Minerals of Stream Sediments from Agunjin Area, Kwara State. World Journal of Applied Science and Technology, 10(1B): 249 – 257.

[41] Schön, J. (2015): Basic Well Logging and Formation Evaluation.

[42] Słota-Valim, M. (2015): Static and Dynamic Elastic Properties, the Cause of the Difference and Conversion Methods–Case Study. Nafta-Gaz, 11, 816-826.

[43] Słota-Valim, M. (2013): Seismic and Well Log Data as a Source for the Calculation of Elastic Properties of Rock Media–Conditioning for Successful Exploration, Well Trajectory, Completion and Production Design of Unconventional Reservoirs. Nafta-Gaz, 69(8): 583--587.

[44] Udo, K. I., Akpabio, I. O. and Umoren, E. B. (2017). Derived Rock Attributes Analysis for Enhanced Reservoir Fluid and Lithology Discrimination. IOSR Journal of Applied Geology and Geophysics (IOSR-JAGG), 5(2): 95-105.

[45] Umoren, E. B., Akankpo, A. O., Udo, K. I., Horsfall, O. I., Atat, J. G. and Asedegbega, J. (2020). Velocity-Induced Pitfalls in Pore Pressure Prediction: Example from Niger Delta Basin, Nigeria. IOSR Journal of Applied Geology and Geophysics, 8(1), 52 – 58.

[46] Umoren, E. B., Uko, E. D., Tamunobereton-Ari, I. and Israel-Cookey, C. (2019). Seismic Velocity Analysis for Improved Geopressure Modelling in Onshore Niger Delta. International Journal of Advanced Geosciences, 7(2), 179-185.

[47] Wang, Y., Han, D. H., Li, H., Zhao, L., Ren, J. and Zhang, Y. (2020): A Comparative Study of the Stress-Dependence of Dynamic and Static Moduli for Sandstones. Geophysics, 85(4): MR179–MR190.

[48] Wang, Y., Han, D., Zhao, L., Li, H. and Long, T. (2022): Static and Dynamic Bulk Moduli of Deepwater Reservoir Sands: Influence of Pressure and Fluid Saturation. Geoscience World (Lithosphere), 1 – 11.

[49] Wentworth, C. K. (1922): A Scale of Grade and Class Terms for Clastic Sediments. Journal of Geology, 30: 377 – 392.

[50] Xu, H., Zhou, W., Xie, R.., Da, L., Xiao, C., Shan, Y. and Zhang, H. (2016): Characterization of Rock Mechanical Properties using Lab Tests and Numerical Interpretation Model of Well Logs. Mathematical Problems in Engineering,

[51] Yang, C. and Liu, J. (2021): Petroleum Rock Mechanics: An Area Worthy of Focus in Geo-energy Research. Advances in Geo-Energy Research, 5(4): 351 – 352.

[52] Zhang, H. (2011): The basic properties of building materials. Woodhead Publishing Limited and Science Press. Pp. 7-423.

[53] Zhang, J. J. and Bentley, L. R. (2005): Factors Determining Poisson's Ratio. CREWES Research Report, 17: 1-15.

[54] Zimmer, M. A. (2004): Seismic Velocities in Unconsolidated Sands: Measurements of Pressure, Sorting, and Compaction Effects, Stanford University.

[55] Zoback, M. D. (2007): Reservoir Geomechanics. Cambridge (UK): Cambridge University Press.